Electronic Supplementary Material (ESI) for RSC Advances.

Supplementary material:

Strain and electric field tunable electronic structure of buckled bismuthene

Ming-Yang Liu[a] Yang Huang[a] Qing-Yuan Chen[a] Ze-Yu Li[a] Chao Cao[b] and Yao He[a]*

[a]*Department of Physics, Yunnan University, Kunming 650091, China*
[b]*Department of Physics, Hangzhou Normal University, Hangzhou 310036, China*

In this Supplementary material, the results using PBE method and relevant dissussion are represented. They may be helpful for understanding the results of PBE+SOC method in main text.

1. The structural parameters of 3D bismuth and b-bismuthene

Table S1 Lattice parameters $a=b$, and c, buckling height h, bond length d, bond angle θ, anisotropy A, cohesive energy E_{coh} of 3D bismuth crystal calculated by usingPBE method.

$a=b$(Å)	c(Å)	h(Å)	d(Å)	θ(deg)	A(%)	E_{coh}(eV/atom)
4.60	12.08	1.62	3.11	95.25	15.7	2.56
4.59[1]	12.03[1]	1.59[1]	3.11[1]			

Table S2 Calculated values of b-bismuthene using PBE method: lattice constants $a_1=a_2$; buckling height h; bond length d; bond angle θ; cohesive energy E_{coh}; band gap E_g; band gap with vdW correction E_{g+vdW}.

$a_1=a_2$(Å)	h(Å)	d(Å)	θ(deg)	E_{coh}(eV)	E_g(eV)	E_{g+vdW} (eV)
4.33	1.73	3.04	90.74	2.44	0.56	0.56
	1.73[1]	3.05[1]			0.55[1]	
	1.73[2]	3.05[2]	90.80[2]		0.55[2]	
4.33[3]	1.71[3]	3.09[3]			0.55[3]	

2. The electronic structure of single b-bismuthene

It has been predicted that the buckled phosphorene,[4] arsenene,[5,6] and antimonene[6,7] are indirect band gap semiconductors, while *b*-bismuthene is direct band gap E_g = 0.56 eV with both the conduction band minimum (CBM) and valence band maximum (VBM) located at the Γ high symmetry point, as seen in Fig. S1. Comparison with the revised calculations based on HSE06 level shows that the PBE band gap can be increased by 0.51 eV. But, the band gap does not be changed when the vdW correction is considered, as list in Table S2. More interestingly, we find that 2D buckled BiAs[8] and BiSb[9] alloys are also direct band gap with the CBM and VBM located at the Γ high symmetry point. According to this finding, under PBE method we deduce that, as the 2D buckled group-V-V BiX (X is other group-V elements) alloy, Bi element has a prominent impact for resulting in the direct band gap. Since the VBM states play an important role in the carrier transport, hence, we further probe into the character of VBM. It is clearly seen from the band structure that the VBM has a strong dispersion, corresponding to a smaller hole effective mass. The VBM mainly originates from p_x and p_y orbitals and forms a σ-like bond on the basis of the density of states and frontier states calculations. As we will see later, the dispersion and frontier states characters of VBM depend sensitively on the in-layer biaxial strain.

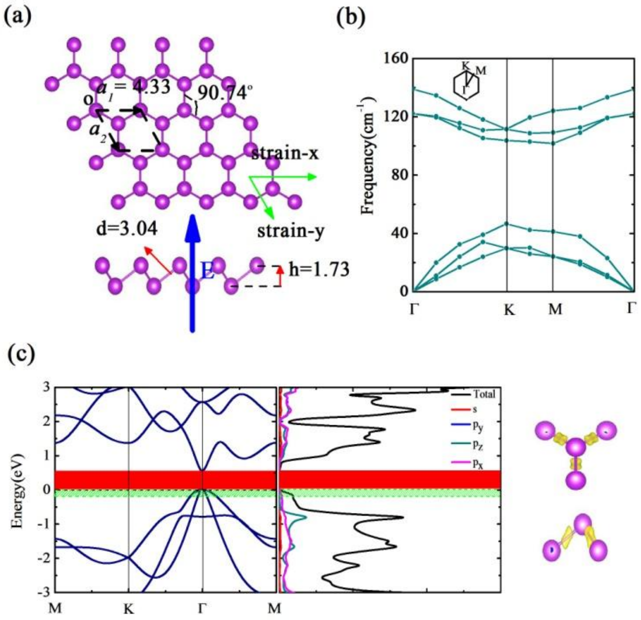

Fig. S1 Calculated results of single *b*-bismuthene using PBE method. (a) Top and side views of the optimized atomic configuration and structural parameters. (b) Phonon dispersion spectrum with PBE optimized parameters. The Brillouin zone is shown by inset. (c) Band structure, density of states, and frontier states character of single *b*-bismuthene. The energy range 0.2 eV below the top of the valence band is green shaded in the band structure and density of states. The band gap is depicted by red range.

3. The electronic structure of bismuthene tuned by in-layer biaxial strain

The in-layer biaxial strain ε is expressed as $\varepsilon = (a-a_0)/a_0$, where a_0 is the lattice constant of the free *b*-bismuthene. Fig. S2 presents four typical strain-tuned *b*-bismuthenes via PBE method. Under the +5% tensile strain, the band structure maintains the direct gap character with E_g = 0.48 eV. It is necessary to point out that the lower energy band near the VBM rises obviously, whereby the character of the frontier states transforms σ-like into $\sigma+\pi$-like mixing bonds. This transition is slightly different from the buckled arsenene in which +5% tensile strain has an entirely π-like character of the frontier states.[10] Compared to the tensile strain, *b*-bismuthene becomes an indirect band gap semiconductor with a 0.31 eV decrease of band gap under the -5% compression strain, since the CBM changes from the Γ high symmetry point to the halfway of Γ-M direction. Actually, the direct-indirect transition has emerged at the compressed strain added up to -3%. There is an attention that the dispersion of VBM with the σ-like bond is stronger than that of free *b*-bismuthene. It is quite natural that the space of the bilayer is stretched and compressed by applying tensile and compressed strain, respectively, and thus the charge overlap altered in the space results in stronger σ-like and weaker π-like bonds. Further increasing the tensile strain up to +10%, *b*-bismuthene is gapless with the VBM and CBM degenerate at the Γ high symmetry point, forming a semimetallic phase. This transition is obtained by a -7% compressive strain as well. These variations of the band structure of *b*-bismuthene in response to the in-layer biaxial strain *e* are similar to those of *b*-arsenene and *b*-antimonene.[5,6,10]

The band gap of *b*-bismuthene as a function of in-layer strain ε under PBE level is presented in Fig. S3. The discussed strain range $-10\% \leq \varepsilon \leq +10\%$ is relatively feasible in experiment. It is suggested clearly that the band gap decreases monotonically with the ε increasing, exhibiting a ‘Λ’-like shape. The variation of band gap is relative smaller at $-3\% \leq \varepsilon \leq +5\%$, whereas it has a rapid reduction beyond -3% and 5% strains. The semiconducting-metallic transition emerges at ε = -7% and +10% and the direct-indirect transition is only induced at ε = -3%.

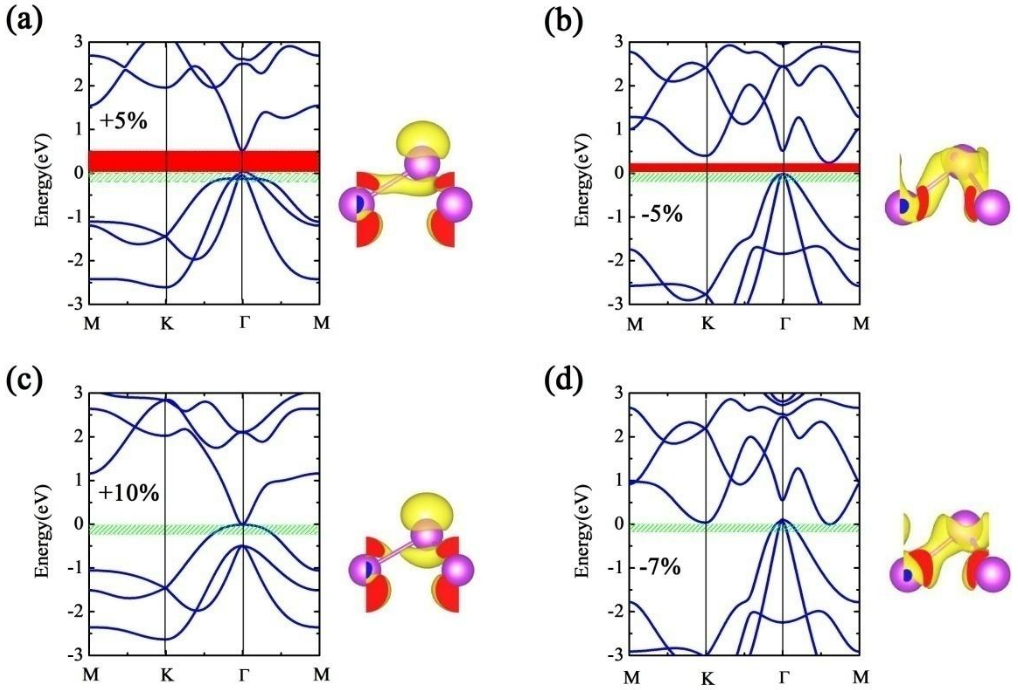

Fig. S2 Calculated band structure and frontier character of (a) +5% tensile strain, (b) -5% compressive strain, (c) +10% tensile strain, and (d) -7% compressive strain. The energy range 0.2 eV below the top of the valence band is green shaded in the band structure. The band gap is depicted by red range.

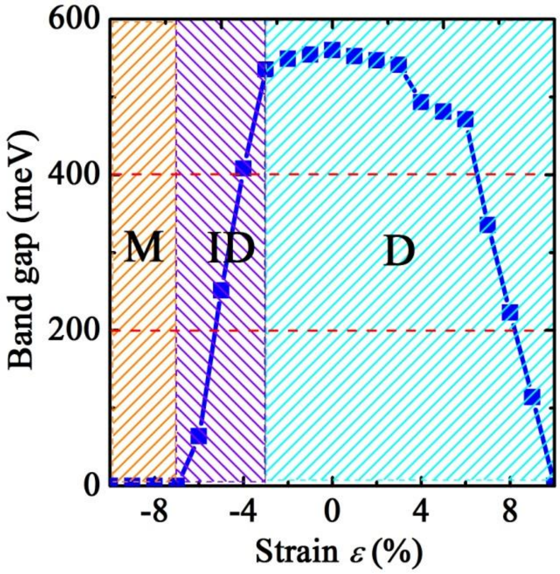

Fig. S3 Strain dependence of the band gap E_g. The insets 'M', 'ID', and 'D' represent metallic, indirect, and direct character, respectively.

We also discuss high tensile strains $\varepsilon > +10\%$ using PBE method. As depicted in Fig. S4(a), it is found that, interestingly, the band structure along the K-Γ direction shows Dirac-type dispersion near the Fermi level forming a novel Dirac cone, while the band opens a gap along the Γ-M direction. The opened gap is 48 and 264 meV with ε = +15% and +20%, respectively. With the ε increasing, the Dirac cone move towards the K high symmetry point and the opened gap gradually increases. The orbital projection analysis suggests that the Dirac cone is derived from the p_z orbital primarily, this is reminiscent of graphene. In fact, the ε added up to a larger value will cause an evidently structural phase deformation. The symmetry group has been changed from C2/M to P-3M1 with free *b*-bismuthene strained by +15% and +20%. This symmetry variation produces the Dirac cone along the high symmetry lines.[11] At the same time, the lone pair of electrons forming π-type band consisted of p_z orbital displays a unique Dirac cone near the Fermi level. Of course, the higher tensile strain is difficult to realize in experiment. We do not find similar Dirac-type dispersion at the same ε including SOC, which can be attributed to the band splitting induced by strong SOC. As seen in Fig. S4(b),the phonon dispersion spectrums confirm that *b*-bismuthene can maintain dynamic stability even at ε = +15%. Robust stability is conductive to investigating the electronic properties of bismuthene at high tensile strain.

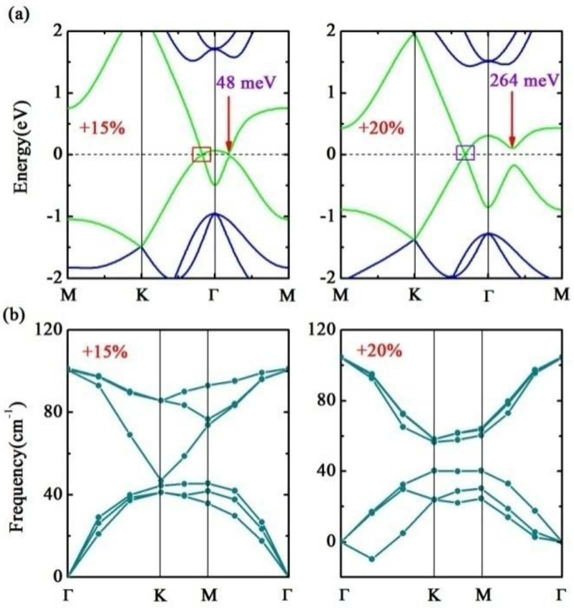

Fig. S4 (a) Band structure and (b) phonon dispersion spectrum of single *b*-bismuthene by applying +15% and +20% in-layer tensile strains under PBE level.

4. Bilayer bismuthene affected by interlayer distance

The optimized AA-stacking bilayer *b*-bismuthene under PBE level is presented in Fig. S5(a). The interlayer distance d_1 is 4.67Å, which is smaller than that of **Ref. 1** 4.80 Å because of including vdW correction. Bilayer *b*-bismuthene is indirect band gap semiconductor owing to the VBM changed to the Γ-K direction with band gap E_g = 0.18 eV (0.28 eV without vdW correction, 0.60 eV using HSE06 method), shown in Fig. S5(b). This direct-indirect transition of going from single to bilayer *b*-bismuthene originates from introducing the interlayer coupling. It is clear that the frontier states of VBM forms π-like character between two single *b*-bismuthene layers due to the interlayer interaction.

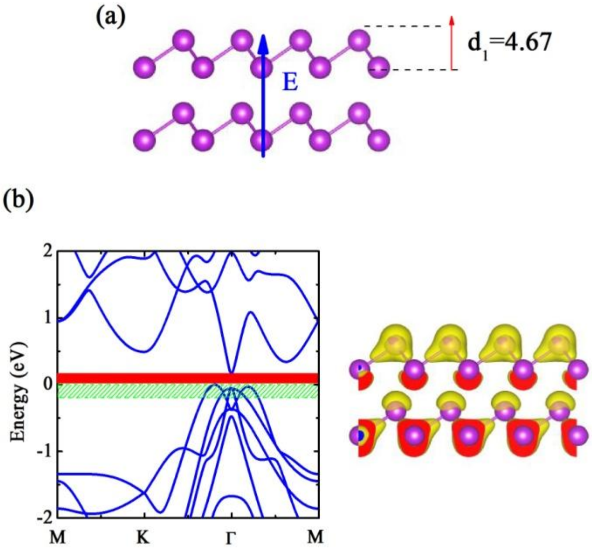

Fig. S5 (a) Side view of the optimized atomic configuration, (b) calculated band structure and frontier states character of the AA-stacking bilayer *b*-bismuthene. The energy range 0.2 eV below the top of the valence band is green shaded in the band structure. The band gap is depicted by red range.

As shown in Fig. S6(a), the band shape of VBM has two obvious contenders, namely located at the Γ high symmetry point and the Γ-K direction, with the interlayer distance variation. 0.2 Å increase and 0.4 Å decrease of the interlayer distance from equilibrium value can lead to indirect-direct band gap and semiconductor-semimetal transition due to the competition of VBM, respectively. There is a very similar band shape between single and bilayer *b*-bismuthene when the interlayer distance adds up to 5.67Å (with band gap 0.33 eV). Actually, the band structure of bilayer *b*-bismuthene gradually tends to the superposition of two single *b*-bismuthenes as the interlayer distance increasing to a large value. The band gap of bilayer *b*-bismuthene as a function of interlayer distance is presented in Fig. S6(b). It can be found that increasing the interlayer distance cannot alter the semiconducting character of bilayer *b*-bismuthene, whereas the semiconducting-semimetallic transition can take place as d_1 deceases to 3.67 Å. These are easy to understand from the charge density variation between two single *b*-bismuthene layers. Notice that the band gap almost retains a monotonic increase within the semiconducting character range except 4.07 to 4.17Å. But, the band gap varies slowly after 5.67 Å, only a tiny change of 20 meV from 5.67 to 7.67Å.

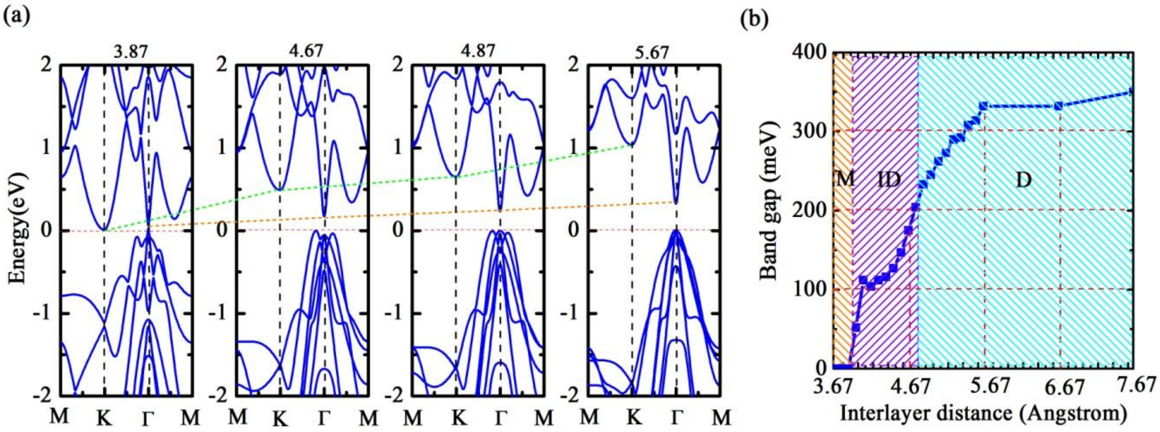

Fig. S6 (a) Band structure of bilayer *b*-bismuthene with four typical interlayer distances 3.87, 4.67, 4.87, and 5.67 Å. (b) Interlayer dependence of the band gap E_g. The insets 'M', 'ID', and 'D' represent metallic, indirect, and direct character, respectively.

5. Single and bilayer bismuthene tuned by electric field

In the *b*-bismuthene, the existence of buckling gives rise to a potential difference between two atomic layers, which turns out to be possible to provide an intrinsic advantage in tuning the electronic structure in terms of a perpendicular electric field.[12] The electric field applying to single and bilayer *b*-bismuthene is also a reasonable method to mimic the interfacial charge transfer effect when the single and bilayer *b*-bismuthene grow on appropriate substrate.[13] We perform the calculations with the strength of electric field ranging from -0.60 to 0.60eV/Å. When the external electric field is small, the band gap of single and bilayer *b*-bismuthene is changed slowly. With increasing the strength of electric field, it has been found that single and bilayer *b*-bismuthene transform semiconductor into metal at the critical electric field E_c = 0.57 and 0.56eV/Å , respectively. These two values of E_c are slightly smaller than that of the buckled arsenene 0.59eV/Å.[9] On the other hand, the negative value of electric field has a nearly consistent effect. The obtained E_c is -0.58 eV/Å and -0.57 eV/Å, repectively. Moreover, in contrast to the buckled arsenene, the direct-indirect band gap transition cannot be found in single and bilayer *b*-bismuthene. In reality, these critical electric fields E_c of inducing electronic phase transition are difficult to realize in experiment, and therefore single and bilayer *b*-bismuthene may be electric robustness.

References

1 E. Aktürk, O. Ü. Aktürk and S. Ciraci, *Phys. Rev. B*, 2016, **94,** 014115.

2 L. Cheng, H. Liu, X. Tan, J. Zhang, J. Wei, H. Lv, J. Shi and X. Tang, *J. Phys. Chem. C*, 2014, **118,** 904.

3 J. Lee, W. C. Tian, W. L. Wang and D. X. Yao, *Sci. Rep.*, 2015, **5,** 11512.

4 Z. Zhu and D. Tománek, *Phys. Rev. Lett.*, 2014, **112,** 176802.

5 C. Kamal and M. Ezawa, *Phys. Rev. B*, 2015, **91,** 085423.

6 S. L. Zhang, Z. Yan, Y. F. Li, Z. F. Chen and H. B. Zeng, *Angew. Chem. Int. Ed. Engl.*, 2015, **54,** 3112.

7 O. Ü. Aktürk, V. O. Özçelik and S. Ciraci, *Phys. Rev. B*, 2015, **91,** 235446.

8 M. Y. Liu, Y. Huang, Q. Y. Chen, C. Cao and Y. He, *Sci. Rep.*, 2016, **6,** 29114.

9 S. Singh and A. H. Romero, *Phys. Rev.* B, 2017, **95,** 165444.

10 Z. Zhu, J. Guan and D. Tománek, *Phys. Rev. B*, 2015, **91**, 161404(R).

11 G. van Miert and C. M. Smith, *Phys. Rev. B*, 2016, **93,** 035401.

12 B. Ghosh, B. Singh, R. Prasad and A. Agarwal, *Phys. Rev. B*, 2016, **94,** 205426.

13 L. Chen, Z. F. Wang and F. Liu, *Phys. Rev. B*, 2013, **87,** 235420.